

# Portable and accurate 3D scanner for breast implants design and reconstructive plastic surgery

C. Rigotti<sup>a</sup>, N. A. Borghese<sup>b</sup>, S. Ferrari<sup>a,b</sup>, G. Baroni<sup>a,c</sup>, G. Ferrigno<sup>a,c</sup>

<sup>a</sup> Politecnico di Milano - Dipartimento di Bioingegneria  
Piazza L. da Vinci, 32 - 20132 Milano, Italy

<sup>b</sup> Laboratory of Human Motion Study and Virtual Reality.  
Istituto Neuroscienze e Bioimmagini - C.N.R.  
Via f.lli Cervi, 93 - 20090 Segrate (Milano) Italy

<sup>c</sup> Centro di Bioingegneria  
Fondazione ProJuventute Don Gnocchi-Politecnico di Milano  
Via Gozzadini, 7 - 20100 Milano, Italy

## ABSTRACT

In order to evaluate the proper breast implant, the surgeon relies on a standard set of measurements manually taken on the subject. This approach does not allow to obtain an accurate reconstruction of the breast shape and asymmetries can easily arise after surgery. Purpose of this work is to present a method which can help the surgeon in the choice of the shape and dimensions of a prosthesis allowing for a perfect symmetry between the prosthesis and the controlateral breast and can be used as a 3D visual feedback in plastic surgery.

The breast 3D shape is reconstructed starting from a set of 3D points which are small spots produced by three optical pens (semiconductor lasers, 670nm, 5mW) manually moved over the breast skin. These spots are surveyed by four specially designed CCD cameras and their 2D position on the camera targets is computed at a sub-pixel accuracy (0.1 pixels) through a real-time cross-correlation implemented on a VLSI custom board (ELITE system). These co-ordinates are sent to a host computer which determines and visualises the 3D position of the points in real-time. Starting from these points, a continuous description of the 3D surface is obtained through a linear combination of weighted Gaussian functions (Radial Basis Network). The weights are estimated through a maximum a-posteriori estimate carried out on a local sub-set of the data points.

Starting from this continuous reconstruction of the surface in 3D space, it is possible to identify the overall volume as well as the shape of whichever section of the breast, which constitute the information needed by the surgeon to evaluate and adapt the proper implant. Moreover, this allows an easy follow up of the skin expansion after the implantation of the expander in the months next to the surgery. The same 3D scanner can be used to get a virtual 3D model of the actual breast which can be interactively modified with the patient in order to achieve a desired shape with aesthetic plastic surgery.

The simplified structure of the system allows to define it as portable and therefore it allows to take measurements easily outside the hospital with very high accuracy. The reconstruction algorithm allows to get 3D reliable data and a compact and easy way to manipulate a virtual model of the breast surface.

Such a system can be of extreme help to assist the surgeon before plastic implants and before corrective plastic surgery. Its main advantages on other methods are the flexibility in terms of size of objects that can be scanned and in the absolutely non contact, non constraining data acquisition procedure and the high accuracy that can be attained.

**Keywords:** RBF network, surface scanning, real time, opto-electronic system, computer graphics, mammary surgery.

## 1. INTRODUCTION

Quantification of physical abnormalities, guiding corrective surgery, plastic surgery, manufacturing of clothing, design of items such as sport and protective equipment or prostheses are some applications in which the mathematical representation of body surfaces and their measurement are essential. Also in the industrial field, surface acquisition applications are numerous. The mathematical description of prototypes represents a key example. In all these fields the object to be

represented cannot be simply expressed as a set of elementary geometric shapes (planes, spherical surfaces, etc.). Only a physical model exists. In order to create a mathematical model of a physical object, one must deal with the problem of the acquisition of the 3D coordinates of several key points with a suitable spatial resolution by means of a coordinate measurement system<sup>1</sup>.

Some techniques, typically using mechanical devices, are characterized by a low flexibility (it is difficult to analyze objects of very different sizes with the same apparatus) and interfere with the object to be described modifying the measure<sup>2</sup>. Ultrasound presents some problems with the low spatial resolution of the image<sup>3</sup>. Opto-electronic systems offer some important advantages, since they do not require any contact with the object, are characterized by great flexibility and moreover are marked by high spatial and temporal resolution.

In this paper, an opto-electronic system for the acquisition of 3D coordinates of surface landmarks is described. It uses a laser beam deflected onto the object to create "virtual" key points. The 3D position of the key points is computed and stored in real-time exploiting the real-time working capability of the system<sup>4</sup>. An on-line three-dimensional graphic representation enrich the system with a visual feedback of the surface being acquired.

The practical application field examined here is plastic surgery and in particular problems related to the mastectomy. A good reconstruction should try to satisfy the patient's wishes and at the same time it should lead to symmetry. The problem is, therefore, the choice of a prosthesis that allows reconstruction of a breast as similar as possible to the other. Up to now this choice is made by manually measuring some key quantities such as the inferior, superior, medial and lateral border of the breast and the distance between the nipples. The system described is able to supply the surgeon not only with the quantities just listed but also with volume, area and shape measures, that are of fundamental importance for an accurate choice of the prosthesis and that cannot be obtained manually.

## 2. METHOD

The sampling of the surface is obtained by the acquisition of the 3D coordinates of one or more laser spots moved across the surface (manually or by a scanner). Figure 1 shows the acquisition system. It includes a laser beam(s), an optional scanning system, the sensors (CCD TV cameras), the system for the coordinate acquisition and a computer for the graphic processing of the 3D data.

Each part of the system is described in the following subsections.

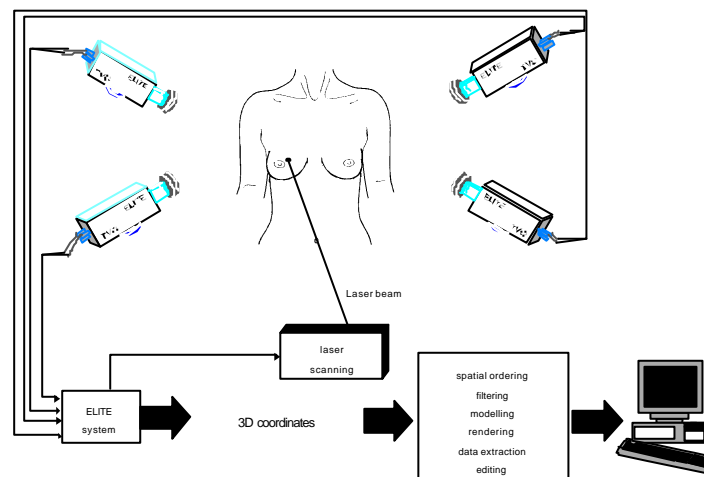


**Figure 1:** The acquisition system. The sampling of the surface is obtained by the acquisition of the 3D coordinates of one or more laser spots produced on the object and suitably displaced (manually or by a scanner). A computer is necessary for the graphic processing of the 3D data.

### 2.1 Laser and scanning system

For the surface scanning a laser beam, directed manually over the surface by an operator, has been used. The source is an array of semi-conductor lasers of 5mW of power and wavelength of 670 nm (a single beam can be used as well). This type of

scanning is useful for the surfaces that are characterized by high spatial frequency content, such as the breast or the face. In this way it is possible to increase the sampling rate in regions with a greater curvature.

It is important to note that the laser beam cross section should be as round as possible (diameter between 5 and 10 mm) to suit the requirements of the acquisition system. Additionally the laser has to be powerful enough to create a high contrast between spot and background, but at the same time it must not injure either patient or operator. A solution has been found using the 5 mW laser while both patient and operator wear protective eye glasses.

Regarding respiration movements, the data acquisition was not synchronized with breathing, firstly because each single respiratory act is not identical repeatable and secondly because if there are 12 breaths in one minute on the average then it should take too long to acquire at least 3000 points. The error, that using a manual scanning procedure is randomly distributed all over the surface, has been calculated as not to be considerable. In fact, using the ELITE system, chest wall displacement has been computed during normal breathing<sup>5</sup>: the average displacement is less than 2 mm, which thanks to its random nature can be greatly reduced by spatial filtering.

## 2.2 ELITE system

The innovative feature of the ELITE system<sup>6</sup> is the marker detection hardware which utilizes the shape and size of the markers rather than only their brightness. This characteristic makes the system easy to use, with respect to others, even in sunlight and is the reason for ELITE's very high measurement accuracy. The architecture of the system is hierarchically organized on two levels.

The lower or first level includes the Interface To the Environment (ITE) and the Fast Processor for Shape Recognition (FPSR). The higher or second level is implemented on a personal computer (IBM AT compatible, with 386, 486 or Pentium processors).

### 2.2.1 First level

The ITE normally includes passive markers of dimensions selected according to the field of view (about 5 mm on a 2 m field of view). These are usually composed of a thin film of retro-reflective paper on plastic hemispheres. To acquire the surface with great accuracy it is necessary to sample a large number of points over the surface. Using traditional markers is therefore impossible: it would take too long to apply them to the surface and the number of samples would be too limited. For this reason passive markers are substituted by a laser beam; the reflection/scattering of the laser on the body is recognized by the system as a marker. Pointing the beam, all the surface is explored and, assuming that the surface is stationary, all the collected coordinates are used to describe mathematically the surface. The TV cameras (solid state CCDs which allow the best definition of the images) with a sampling rate of 100 Hz also belong to the ITE.

The second block of the first level, the FPSR, constitutes the core of the system and performs the recognition of the markers and the computation of their coordinates. The FPSR computes in real time a two-dimensional cross-correlation between the incoming digitized signal and a reference mask and drives the ITE with synchronization signals. The mask is a 6x6 pixel matrix and is designed to achieve a high correlation with the marker shape and a low one with the background<sup>7</sup>:

-8	-8	-8	-8	-8	-8
-8	0	1	1	0	-8
-8	1	7	7	1	-8
-8	1	7	7	1	-8
-8	0	1	1	0	-8
-8	-8	-8	-8	-8	-8

After correlation, the first level sends to the computer the 2D coordinates of the over threshold pixels as recorded during the acquisition of the subject.

### 2.2.2 Second level

The second level performs a high level processing: 2D calibration (camera calibration), 3D intersection and further processing such as filtering, derivatives computing, modeling, etc. Between the first and the second level (albeit software implemented in the computer) a further step is carried out. By using a coordinate enhancement algorithm, taking into account the cross-

correlation function, the 2D resolution is increased to 1/65000 of the field of view<sup>6</sup>. This is achieved by computing the center of gravity ( $x_c$  and  $y_c$ ) of the over-threshold pixels (of coordinates  $x_{i,j}$  and  $y_{i,j}$ ) belonging to the same marker weighted by the cross-correlation value ( $R_{i,j}$ ) as follows:

$$x_c = \frac{\sum_{i,j} x_{i,j} R_{i,j}}{\sum_{i,j} R_{i,j}} \quad \text{and} \quad y_c = \frac{\sum_{i,j} y_{i,j} R_{i,j}}{\sum_{i,j} R_{i,j}} \quad (1)$$

This processing relies on the fact that the closer it is the pixel to the true marker center, the higher is the value of the cross-correlation function.

### 2.2.2.1 System calibration

The system calibration consist of two steps required to achieve 3D reconstruction (space intersection): camera calibration and space resection (localization of cameras in space). The accuracy in this phase is very important as it influences the subsequent processing of the acquired data.

The collinearity equations represent a mathematical model of the cameras which relates the 2D target coordinates of marker projection, the 3D coordinates of the marker in the space and the stereophotogrammetric parameters (the six spatial camera coordinates and its three internal parameters)<sup>8</sup>.

$$x - x_0 = -c \frac{m_{11} (X - X_0) + m_{12} (Y - Y_0) + m_{13} (Z - Z_0)}{m_{31} (X - X_0) + m_{32} (Y - Y_0) + m_{33} (Z - Z_0)} \quad (2a)$$

$$y - y_0 = -c \frac{m_{21} (X - X_0) + m_{22} (Y - Y_0) + m_{23} (Z - Z_0)}{m_{31} (X - X_0) + m_{32} (Y - Y_0) + m_{33} (Z - Z_0)} \quad (2b)$$

with:

$X_0, Y_0, Z_0$  - TV camera location (3D coordinates of the perspective center);

$m_{i,j}$  - nine director cosines, which are function of the camera rotation angles with respect to an absolute reference system:  $\Omega$ ,

$\Phi, K$  (pitch, yaw, roll);

$x_0, y_0$  - TV camera principal point coordinates (intersection of optical axis and image plane);

$c$  - focal length;

$X, Y, Z$  - 3D coordinates of the surveyed point;

$x, y$  - 2D target coordinates of its projection,

$X_0, Y_0, Z_0, \Omega, \Phi, K$  are named external geometrical parameters,  $x_0, y_0$  and  $c$  inner parameters.

In the real situation, we must take into account the quantization error (stochastic) introduced by the measuring system and the optical distortions (systematic error).

Our approach to space resection, in order to determine the geometrical parameters in equations (2), is based on the classical iterative least-squares estimation extended to the inner parameters which allows the maximum freedom in TV cameras positioning and setting. By surveying a set of points of known coordinates (control points of coordinates  $X, Y, Z$ ), it is possible to write the couple of equations 2a and 2b for each of them. All these  $2N$  equations (with  $N$  equal to the number of control points) can be arranged in a non linear system, which can be solved after a linearization around a suitable starting point. Each couple of equations will have the following form:

$$f_1(X_0, Y_0, Z_0, \mathbf{w}, \mathbf{j}, \mathbf{k}, x_0, y_0, z_0) = 0 \quad (3a)$$

$$f_2(X_0, Y_0, Z_0, \mathbf{w}, \mathbf{j}, \mathbf{k}, x_0, y_0, z_0) = 0 \quad (3b)$$

The starting point  $P_i = (\overline{X_0}, \overline{Y_0}, \overline{Z_0}, \overline{\mathbf{w}}, \overline{\mathbf{j}}, \overline{\mathbf{k}}, \overline{x_0}, \overline{y_0}, \overline{z_0})$  is obtained by rough estimation from the experimental set-up. The linearized equations have the form:

$$f_1(P_i) + \frac{df_1}{dX_0} \Big|_{P_i} \Delta X_0 + \frac{df_1}{dY_0} \Big|_{P_i} \Delta Y_0 + \frac{df_1}{dZ_0} \Big|_{P_i} \Delta Z_0 + \frac{df_1}{d\mathbf{w}} \Big|_{P_i} \Delta \mathbf{w} + \frac{df_1}{d\mathbf{j}} \Big|_{P_i} \Delta \mathbf{j} + \frac{df_1}{d\mathbf{k}} \Big|_{P_i} \Delta \mathbf{k} + \frac{df_1}{dx_0} \Big|_{P_i} \Delta x_0 + \frac{df_1}{dy_0} \Big|_{P_i} \Delta y_0 + \frac{df_1}{dz_0} \Big|_{P_i} \Delta z_0 = 0 \quad (4a)$$

$$f_2(P_i) + \frac{df_2}{dX_0} \Big|_{P_i} \Delta X_0 + \frac{df_2}{dY_0} \Big|_{P_i} \Delta Y_0 + \frac{df_2}{dZ_0} \Big|_{P_i} \Delta Z_0 + \frac{df_2}{d\mathbf{w}} \Big|_{P_i} \Delta \mathbf{w} + \frac{df_2}{d\mathbf{j}} \Big|_{P_i} \Delta \mathbf{j} + \frac{df_2}{d\mathbf{k}} \Big|_{P_i} \Delta \mathbf{k} + \frac{df_2}{dx_0} \Big|_{P_i} \Delta x_0 + \frac{df_2}{dy_0} \Big|_{P_i} \Delta y_0 + \frac{df_2}{dz_0} \Big|_{P_i} \Delta z_0 = 0 \quad (4b)$$

These form a 2N linear equation system in 9 unknowns. It can be solved by least squares technique leading to a solution vector  $\Delta P_i = (\Delta X_0, \Delta Y_0, \Delta Z_0, \Delta \mathbf{w}, \Delta \mathbf{j}, \Delta \mathbf{k}, \Delta x_0, \Delta y_0, \Delta z_0)$ . The new starting point is computed as  $P_{i+1} = P_i + \Delta P_i$ . The procedure is repeated until  $\Delta P_k$  is lower than a preset threshold<sup>9</sup>. In order to obtain the number of control points required (at least 5 not lying on a plane), without having to spend much time to compute their 3D coordinates, the control points have been located on a plane grid, which is shifted according to reference locations placed on the floor. Very precise measurements are required only once, when the markers are put on the grid and the references on the floor are located, so every time that the system set-up has to be changed, little time is required to calibrate it.

The determination of the parameters for the correction of the optical distortion errors (the image of a square put in front of the camera appears as a curvilinear quadrilateral), is realized with the acquisition of a grid of markers, the geometry of which is known, located in a plane parallel to the sensor and at such a distance as to fill it. By the deformation of the meshes of the grid, the coefficients of suitable quadratic functions are computed. These functions applied to the points of each mesh compensate the deformation<sup>9</sup>.

Corrected (undistorted) coordinates  $x_u, y_u$  are obtained by the following equations:

$$x_u = a_{xi} + b_{xi} + c_{xi}x^2 + d_{xi}xy + e_{xi}y^2 + f_{xi} \quad (5a)$$

$$y_u = a_{yi} + b_{yi} + c_{yi}x^2 + d_{yi}xy + e_{yi}y^2 + f_{yi} \quad (5b)$$

Parameters  $a_{xi}, b_{xi}, c_{xi}, d_{xi}, e_{xi}, f_{xi}, a_{yi}, b_{yi}, c_{yi}, d_{yi}, e_{yi}, f_{yi}$  are computed, for each mesh  $i$ , by a transformation that replaces the distorted vertices ( $V_{ji}, j=1,2,3,4$ ) with the reference undistorted ones ( $V_{uji}$ ), transforming the straight lines joining two vertices into straight lines and internal and external points with respect to these lines again in internal and external points.

This type of calibration can be referred as virtual rather than physical; in fact the distance between the grid and the camera, grid dimension and focal length are not known. The coordinates are expressed in pixels and not in target physical units.

Once the stereophotogrammetric parameters have been estimated, space intersection can be carried out. The two straight lines conveyed through the cameras perspective centers and 2D image projection<sup>10</sup> are considered ( $r$  and  $s$  in figure 2). The coordinates of the middle point of the minimum distance segment between the lines are assumed to be the coordinates of the reconstructed point. The director cosines of  $r$  and  $s$  are computed by the coordinates of the projected point  $x_i, y_i$  and the focal length  $c_i$  as follows:

$$l'_1 = \frac{x_i - x_{0i}}{\sqrt{(x_i - x_{0i})^2 + (y_i - y_{0i})^2 + (z_i - c_i)^2}} \quad (6a)$$

$$l'_2 = \frac{y_i - y_{0i}}{\sqrt{(x_i - x_{0i})^2 + (y_i - y_{0i})^2 + (z_i - c_i)^2}} \quad (6b)$$

$$l'_3 = \frac{z_i - z_{0i}}{\sqrt{(x_i - x_{0i})^2 + (y_i - y_{0i})^2 + (z_i - c_i)^2}} \quad (6c)$$

$$\begin{bmatrix} l_1 & l_2 & l_3 \end{bmatrix}^T = M_i \begin{bmatrix} l'_1 & l'_2 & l'_3 \end{bmatrix}^T \quad (6d)$$

where  $M_i$  is the rotation matrix obtained from the angles  $\omega_i$ ,  $\phi_i$ ,  $\kappa_i$ . Since  $r$  and  $s$  respectively pass through  $c_1$  of coordinates  $X_{01}, Y_{01}, Z_{01}$  and  $c_2$  of coordinates  $X_{02}, Y_{02}, Z_{02}$ , it is straightforward to write their equations and to find the segment of minimum distance joining them.

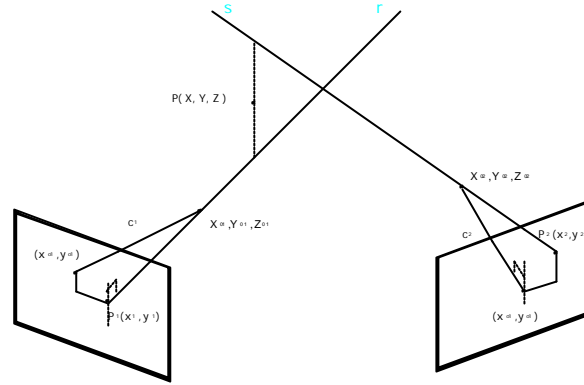


**Figure 2:** Space intersection. The two straight lines conveyed through the camera's perspective centers and 2D image projection are considered; the coordinates of the middle point of the minimum distance segment between the lines are assumed to be the coordinates of the reconstructed point.

The system local accuracy has been evaluated and the maximum error found with respect to the true value was 1/24000 of the diagonal<sup>11</sup> of the calibrated volume.

The last part of the system, the data processing, will be described after the experimental set-up section.

### 2.3 Real time

The presented system is based on the real-time capabilities of the ELITE motion analyzer. Real-time features were obtained by exploiting the features of the interfacing between the two levels of the system architecture based on a Direct Memory Access (DMA) data transfer, in order to implement true real-time acquisition, processing and representation of two-dimensional and three-dimensional kinematics data. Philosophy of real-time operation consists of performing the basic elaboration at the second system level (centroid calculation, 3D reconstruction, graphic representation) on the raw data belonging to a frame already transferred from the first level, while the background DMA process writes in memory the information relative to the successive frames. The method guarantees in any case the complete execution of the necessary elaboration, updating the start of the successive processing at the beginning of the most recent acquired frame. In this way, real-time characteristic is always maintained, even engaging the processing unit in any desired operation, with the only consequence of the eventual loss of intermediate frames, i.e. a decrease of the actual acquisition sampling rate.

Performance of the system working in real-time turn out to fulfill the requirements of the presented application. Requiring a 3D graphic representation on 3 planes and contemporary data saving on HD through a previously allocated Extended Memory buffer, up to 12 markers could be seen by 4 TV cameras, maintaining the nominal system sample rate of 100 Hz<sup>4</sup>.

### 2.4 Experimental set-up

As sketched in Fig.1, in the experiments four TV cameras have been placed in front of the subject. A camera pair has been arranged vertically on the right side, the other on the left side, in order to allow a good visibility of the surface by at least two cameras.

The surface has been scanned by using the manual approach cited above. The time required to explore the surface is an important parameter in the definition of the experimental set-up and it is particularly critical because of the chest movement due to breathing.

With a time of 30 seconds, three lasers and 100 Hz sampling rate, 9000 points have been acquired.

During the acquisition the subject was in a sitting position.

### 2.5 Reconstruction through Hierarchical Radial Basis Function Networks

The reconstruction of the breast 3D surface from the set of unorganized points obtained from the acquisition can be seen as a more general problem of function approximation where the function to be approximated is the 3D surface of the breast (Figure3). As there is not a good general model of the breast shape, a solution is to resort to non-parametric estimate. In particular, due to their generalisation capabilities, Artificial Neural Networks (ANN), and, more recently, Radial Basis Functions (RBF) networks, have been proposed as general approximators<sup>12</sup>. In the following we will show that these computational models can be extremely effective in the reliable reconstruction of the 3D breast surface of very different shapes.

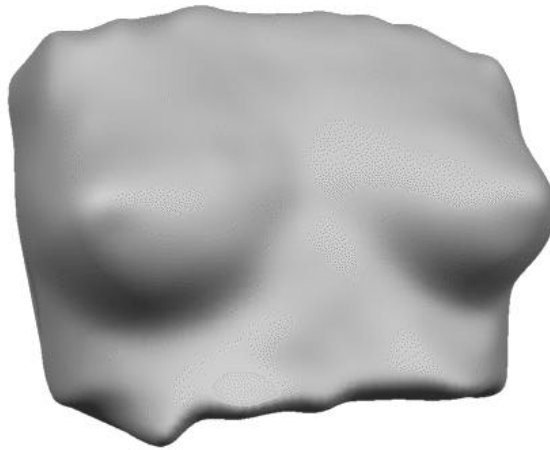


**Figure 3:** The reconstructed breast surface

A RBF network with Gaussian elements has the following analytical shape:

$$s(\mathbf{x}) = \sum_{k=1}^M \mathbf{w}_k g(\mathbf{x}; \mathbf{c}_k, \mathbf{S}_k) \quad (7)$$

where  $M$  is the number of units forming the network, and the sets  $\mathbf{c}_k$ ,  $\mathbf{S}_k$  and  $\mathbf{w}_k$  are respectively the positions, the covariance and the weights assigned to each Gaussian element and  $g(\cdot)$  is the Gauss function.

The above parameters can be subdivided into two sets: the *structural parameters* ( $M$ ,  $\mathbf{c}_k$ ,  $\mathbf{S}_k$ ), and the *synaptic weights*  $\mathbf{w}_k$ . These two sets can be determined separately. In fact, the Gaussian centers,  $\mathbf{c}_k$ , are positioned on a regular grid, and by keeping the variance of the elements equal, equation (7) can be seen as a linear filter. Moreover, when normalized Gaussians are employed, Equation (7) can be written, over only one dimension, as follows:

$$s(x) = \sum_{k=1}^M w_k \frac{e^{-\frac{(x-c_k)^2}{s^2}}}{\sqrt{\pi s}} = \sum_{k=1}^M s_k \Delta x \frac{e^{-\frac{(x-c_k)^2}{s^2}}}{\sqrt{\pi s}} \quad (8)$$

where  $\Delta x$  is the spacing between two Gaussians and  $s_k$  is the value of  $s(x)$  in the grid crossing. Assuming  $w_k = s_k \Delta x$  the values of  $S(x)$  approximate the data points in  $s_k$ <sup>14</sup>. To determine the proper value of  $\sigma$ , linear filtering theory can be applied. The cut-off frequency of the Gaussian is regulated by the value of  $\sigma$ : the larger is  $\sigma$  the smaller is the cut-off frequency and viceversa. In order to get  $s(x)$  close enough to the real function,  $\sigma$  should be small enough to get a cut-off frequency larger than the maximum frequency constant of the function to be reconstructed. However  $\sigma$  should not be too large to avoid aliasing, and the following empirical relationship is obtained<sup>13</sup>:

$$2 \Delta x \frac{\sqrt{-\ln \delta_2}}{\pi} \leq \sigma \leq \frac{\sqrt{-\ln \delta_1}}{\pi v_M} \quad (9)$$

This equation sets the constraint on the choice of the value of  $s$  as a function of the maximum cut-off frequency  $n_M$  and spacing between two Gaussians.  $\delta_1$  and  $\delta_2$  represent the minimum accepted amplitude of the frequency response in the Pass Band and the maximum amplitude in the Stop Band.

This method can be applicable also when the control points are not equally spaced as in the data points got from the acquisition. In this case a local maximum a-posteriori estimate of the distortions at the grid crossing can be carried out using a local Maximum A-Posteriori estimate:

$$s(c_k) = \frac{\sum_{x_r \in R} s(x_r) e^{-\frac{(x_r - c_k)^2}{\sigma_w^2}}}{\sum_{x_r \in R} e^{-\frac{(x_r - c_k)^2}{\sigma_w^2}}} \quad (10)$$

where the region R is taken somehow arbitrary as that included inside two grid meshes:  $R : c_k \pm \Delta c$  ( $\Delta c = c_{k+1} - c_k$ ). The value of  $\sigma_w$  has been taken equal to  $s/2$  to avoid additional filtering of the data. This choice is based on the observation that the closer is a control point to  $s_k$ , the closer is its height to that measurable in the point  $c_k$ . This suggest to weight the data points in the neighbourhood of  $c_k$  by a function decreasing with the distance of that point from  $s_k$ . Assuming the weighting function Gaussian, the MAP estimator is obtained<sup>12</sup>.

This approach is somehow rigid as it allows only one value for the variance (and for the cut-off frequency) over all the input space: this should be chosen small enough to reconstruct the finest details, although these may occur in few regions of the input space. The consequence is a dense packing of the Gaussian units with a loss of resources and possibly overfitting. A better solution is to distribute more Gaussian units in those regions where they are effectively required (higher spatial frequencies) and to use less Gaussians in the other breast regions. This has been achieved using a two-layer approach, each layer having its own grid spacing and a characteristic variance. The first layer will output an approximation of the breast surface at a high scale (large value of  $s$ ). The second layer will contribute by adding a more detailed reconstruction of those areas with higher spatial frequencies. This second level is therefore not complete but shows clusters of Gaussians in these regions. The Gaussians are inserted automatically by monitoring the residual error. This is defined as:

$$r = \sum_{k=1}^R |r_k| \quad (11)$$

where  $r_k$  is the distance between the height of the surface in the point  $x_k$  and the height reconstructed by the network in that point. A Gaussian is inserted in a point  $x_k$  only when its residual error is greater than the quantization error associated with the acquisition. It should be remarked that with this kind of architecture, the obtained residual error is lowered uniformly under the quantisation error determining the parameters directly from the input data set.

### 3. RESULTS



The more innovative capability of this method is volume computation which is currently entrusted to the surgeon experience (Figure 4).

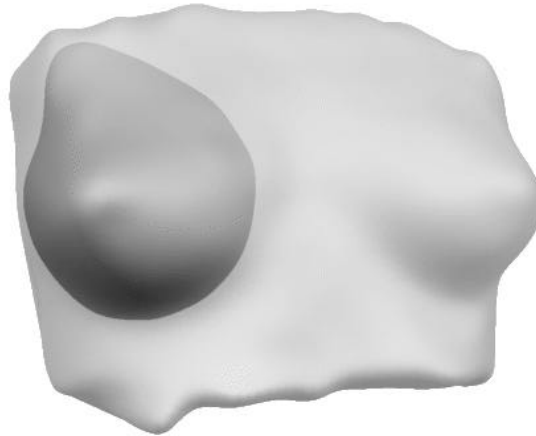


**Figure 4:**The volume computation. Once the surface has been reconstructed, it is possible to compute the volume of region of interest on the surface, in this case the region of the breast

The accuracy of the estimate of the volume has been tested on 7 female subjects. The volume as been computed with an error of 4.3% on the average. The reference volume has been calculated by measuring the volume of the water displaced in a graduated vessel (accuracy of 10 ml) in which the breast was immersed.

As to the linear measures, they have been estimated on the subjects with traditional (manual) measuring techniques. For the segment measure the error is of 2% on the average; for the measure on the surface topography the error is of 5% on the average. These errors can not be imputed at all to our measurement system because also traditional methods are prone to errors and however the measurements were taken in different times including size variation due to rib cage expansion. This method presents some advantages with respect to the other methods proposed for the evaluation of volumes in mammary reconstruction.

The device presented by Cutting and al.<sup>15</sup> (Echo scanner manufactured by Cyberware Laboratories) is not as flexible and it is cumbersome. A low-energy laser light beam is passed through a cylindrical lens so that a vertical line is projected on the surface. A video camera records the image of this line from a fixed angle to the light source. The mechanical relationship between camera and projector is critical for the data accuracy and however no data on accuracy are given at all.

Loughry et al.<sup>16</sup> presented a measurement technique that used close-range stereophotogrammetry to characterize the shape of the breast. Wide-angle stereometric cameras were used for precise metric-quality imagery combined with an optical projector. Again no data were provided about accuracy or calibration burden.

Bathia et al.<sup>17</sup> presented a study to compute the three dimensional surface changes that accompany facial surgical procedures. An optical three dimensional scanner with 360 degree surface coverage of the subject's head and a sub-second data acquisition was used. The scanner used six pairs of white light pattern projectors and digital TV cameras. The accuracy was poor: for an injected volume of 2 cc, in three different measurements 1.7 cc, 2.9 cc and 2.7 cc were obtained.

All these approaches did not enter in the clinical practice, may be because of their low accuracy, difficult of use and high cost. The approach presented in this paper could have some chances in the first two parts, while the cost is still high and could be justified only by an intensive use of the system itself.

#### 4. DISCUSSION AND CONCLUSION

A new method has been presented for the measurement of distances, areas and volumes of the breast in plastic surgery. The accuracy of the system is very high and the tests performed have confirmed it, although the reference taken wasn't reliable enough for a true comparison.

This method could represent a starting point for the design of new expanders and new prostheses. Till now the industries receive inputs for the project only from the surgeon. As the reconstruction techniques are becoming more and more accurate and, as the patients are becoming more and more demanding in term of symmetry, it is necessary a diversification of the prosthesis implants.

This system could be the tool for a statistical analysis of the breast shape that could provide a set of objective data representing a starting point for the design of a new type of prostheses.

## 5. REFERENCES

1. A. Aliverti, G. Ferrigno and A. Pedotti, "Surface analysis by laser beam scanning and stereophotogrammetry", *Proc. SPIE* **2067**, 209-219 (1993).
2. H.R. Nicholls and M.H. Lee, "Analysing data produced by tactile sensors", Chap.11 in *Automation, Production Systems and Computer-Integrated Manufacturing Robot technology*, M. Groover Ed., Prentice Hall (1986).
3. H. Urban, "Ultrasonic Imaging for industrial scene analysis", in *Sensor Devices and System for Robotics*, NATO ASI series, Computer and System Sciences, Alicia Casals (ed.), **52**, pp. 187-194, Springer Verlag (1989).
4. G. Baroni, G. Ferrigno "Real time motion analysis by means of passive markers", in *Proceedings of XVI<sup>th</sup> World ISB Congress*. Tokyo, p. 1 (1997)
5. P. Carnevali, G. Ferrigno, A. Aliverti and A. Pedotti, "A new method for 3D optical analysis of chest wall motion", *Technology and Health Care* **4**(1), 43-65 (1996).
6. G. Ferrigno and A. Pedotti, "ELITE: a digital dedicated hardware system for movement analysis via real-time TV signal processing", *IEEE Trans. Biomed. Eng. (BME)*, **32**, 943-950 (1985).
7. G. Ferrigno and A. Pedotti, "Modularly expansible system for real-time processing of a TV display, useful in particular for the acquisition of coordinates of known shapes objects", *US Patent No. 4,706,296* (1987).
8. P.R. Wolf, "Elements of photogrammetry", 1974, *McGraw-Hill, New York*.
9. G. Ferrigno, N.A. Borghese and A. Pedotti, "Pattern recognition in 3D automatic motion analysis", *ISPRS J. Photogramm. Remote Sensing*, **45**, 227-246 (1990).
10. N.A. Borghese and G. Ferrigno, "An Algorithm for 3D Automatic Movement Detection by means of standard TV cameras", *IEEE Trans. Biomed. Eng. (BME)* **37**, 1221-1225 (1990).
11. A. Pedotti and G. Ferrigno, "Opto-electronic based system", in *Three dimensional analysis of human movement*, P. Allard, I.A.F. Stokes and J.P. Bianchi, pp. 57-77, Human Kinetics Publishers (1995).
12. F. Girosi, M. Jones and T. Poggio, Regularization theory and Neural Networks Architectures, *Neural Computation* **7**. pp. 219-269, 1995
13. N.A. Borghese and S. Ferrari, *Hierarchical RBF networks and local parameter estimate*, in press in NeuroComputing.
14. A.V. Oppenheim and R.W. Shafer, *Digital Signal Processing* (Prentice-Hall, Englewood Cliffs, NJ, USA, 1987).
15. C. Cutting, J. McCarthy, D. Karron, "Three-dimensional input of body surface data using a laser light scanner", *Ann. Plast. Surg.* **21**(1), pp. 38-45 (1988).
16. W. Loughry, D. Sheffer, T. Price, M. Lackney, R. Bartfai, W. Morek, "Breast volume measurement of 248 women using biostereometric analysis", *Plast. Reconstr. Surg.*, **80**(4), pp. 553-558 (1987).
17. G. Bathia, M. Vannier, K. Smith, P. Commean, J. Riolo, L. Young, "Quantification of facial surface change using a structured light scanner", *Plast. Reconstr. Surg.*, **94**(6), pp.768-774 (1994).